Enhanced wake mixing in wind farms using the Helix approach: A loads sensitivity study

Aemilius A.W. van Vondelen[1], Sachin T. Navalkar[2], Daan R.H. Kerssemakers[1],
and Jan-Willem van Wingerden[1]

Abstract— The Helix approach is a control technology that reduces the wake effect in wind farms by accelerating wake mixing through individual pitch control, resulting in significant AEP gain. However, this study found that depending on its settings, the controller may increase pitch bearing damage and loads on some turbine components. Using a modified version of NREL's Reference OpenSource Controller in OpenFAST, this study analysed the sensitivity of loads and pitch bearing damage to different Helix controller settings on the IEA-15MW reference offshore wind turbine. Results showed that loads increased with the excitation signal amplitude but were less affected by its frequency. Additionally, more pitch bearing damage was observed in the counterclockwise Helix direction, while slightly higher loads were observed in the clockwise direction when using the same excitation signal amplitude and frequency for both directions.

I. INTRODUCTION

The Netherlands committed to obtaining all of its energy from renewable sources by 2050 [1]. Due to shallow waters and strong winds in the Dutch North Sea, offshore wind will play a large role in this transition. Recently, this was confirmed by doubling the desired capacity for 2030 to 21 GW [2]. Even though the cost per kWh of offshore wind energy is already on par with fossil fuels, lowering the cost further will expedite the transition. Technological innovation in wind engineering is expected to contribute significantly to this, and one important open challenge that demands innovation is a disturbing phenomenon called the wake effect.

The wake is a low-velocity flow region downwind of a turbine, which propagates further downwind until it becomes unstable and mixes again with the surrounding ambient wind flow [3]. If a downstream wind turbine is (partly) aligned with the wake of an upstream wind turbine, it experiences a lower wind velocity and yields a lower power output [4]. Moreover, due to increased turbulence and partial wake overlap, the downstream turbine also experiences higher loads [5]. For that reason, mitigating the wake effect plays a large role in wind farm layout optimization [6], [7]. In spite of that, the power losses due to the wake effect can be as high as 20% for some wind farms [8].

The field that attempts to mitigate this effect using control is called wind farm control (WFC). A recent study inves-

tigated the main motivations for wind farm control where a survey was passed amongst stakeholders from academia, industry, and other fields [9]. The most important benefit of WFC was found to be the increase in energy production, whereas load reduction came second. Traditionally, these two objectives contradict, as higher production generally involves higher wind speeds and thus higher loads. However, WFC aims at optimizing both objectives on a farm level.

One popular technique in WFC that received much attention is wake steering [10], [11]. This approach employs a farm-wide super controller that intentionally misaligns upstream turbines with respect to the dominant wind direction such that their wakes are steered to pass on one side of the downstream turbine. Another technique involves derating upstream turbines such that more energy can be drawn by downstream turbines. However, the effectiveness of this method is still a topic of discussion as some studies haven't found significant increases in performance [12], [13].

The above-mentioned techniques aim to find a steady-state optimum for a given environmental condition. Other techniques were proposed that introduce dynamics to initiate earlier mixing of the wake with the ambient wind flow. One method called Dynamic Induction Control (DIC) imposes a low-frequent sinusoidal signal on the collective pitch actuators causing a periodically varying thrust force improving wake mixing significantly [14]–[16]. The parameter that governs the frequency of this signal is the dimensionless Strouhal number, whose optimal setting was found experimentally [17]. These results show great potential for this technique. However, a notable disadvantage is that the pulsing thrust causes significant loads on the blades and tower base, reducing fatigue life substantially [18].

Recently, the Helix approach was proposed which uses individual pitch control (IPC) to initiate early wake mixing [19]. Similar to DIC, the Helix method imposes sinusoids on the blade pitch actuators and is governed by the Strouhal number. However, by imposing out-of-phase pitch actuation signals on the individual blades, a helix-shaped wake is created behind the turbine which enhances wake mixing. Initial simulations demonstrated that, as the wake breaks down earlier, the power production of a two-turbine wind farm was increased by up to 7.5%, and thrust fluctuations (and loads resulting from this) are significantly lower when using this method compared to DIC [18], [19].

Being a relatively new approach, no quantitative investigation has been done in the optimal settings of the Helix control method balancing fatigue stress with energy gain.

[1]Aemilius A.W. van Vondelen, Daan R.H. Kerssemakers, and Jan-Willem van Wingerden are with the Delft Centre for Systems and Control, Delft University of Technology, 2628 CD Delft, The Netherlands A.A.W.vanVondelen@tudelft.nl
[2]Sachin T. Navalkar is with Siemens Gamesa Renewable Energy, Prinses Beatrixlaan 800, 2595 BN The Hague, The Netherlands

This study aims to complete the first part.

The main contribution of this paper is a loads sensitivity analysis for the Strouhal number and signal amplitude which can be used as a precursor for high-fidelity large-eddy simulation (LES) farm studies where the power production of the downstream turbine can be measured. At this stage, only fatigue loads during normal power production (IEC-6100-3, DLC 1.2 [20]) are considered, as, under Helix control, turbine operation is largely within its normal operational envelope, and the response to extreme events is not expected to be significantly different.

The remainder of this paper is organized as follows. Section 2 describes the theoretical background of the Helix approach and loads analysis. Section 3 presents the simulation setup. The results are presented in Section 4 and the paper is concluded in Section 5.

II. THEORETICAL BACKGROUND

This section introduces the underlying principle of the Helix. Next, the fatigue analysis methodology is described, followed by the pitch bearing damage quantification.

A. The Helix approach

The Helix approach is an open-loop wake mixing control method that uses the individual pitch actuators of the blades of a wind turbine. Similar to IPC for load reduction [21], [22], it uses the Multi-Blade Coordinate (MBC) transform [23]. This coordinate transformation maps the rotating coordinate system of the individual blades to the non-rotating coordinate system. Thereby, this transformation decouples the blade root bending moments, $M_i(t)$ for $i = 1, 2, 3$, to a collective moment M_0, a moment around the tilting axis M_{tilt} and a moment around the yawing axis M_{yaw} using the azimuth ψ_i of each blade $i = 1, 2, 3$:

$$\begin{bmatrix} M_0(t) \\ M_{\text{tilt}}(t) \\ M_{\text{yaw}}(t) \end{bmatrix} = \frac{2}{3} \begin{bmatrix} 0.5 & 0.5 & 0.5 \\ \cos(\psi_1) & \cos(\psi_2) & \cos(\psi_3) \\ \sin(\psi_1) & \sin(\psi_2) & \sin(\psi_3) \end{bmatrix} \begin{bmatrix} M_1(t) \\ M_2(t) \\ M_3(t) \end{bmatrix}. \tag{1}$$

Traditionally speaking, straightforward SISO PID control can then be used for load reduction, while collective pitch can be controlled using the baseline pitch controller. Note that in practice, actuator delays might prevent full decoupling, and an additional correction is required [24].

The Helix approach, being open-loop, only imposes a signal on the tilt and yaw inputs, θ_{tilt} and θ_{yaw}, which are translated to inputs for the pitch actuators in the rotating frame using the following 'reverse' MBC transform:

$$\begin{bmatrix} \theta_1(t) \\ \theta_2(t) \\ \theta_3(t) \end{bmatrix} = \begin{bmatrix} 1 & \cos(\psi_1) & \sin(\psi_1) \\ 1 & \cos(\psi_2) & \sin(\psi_2) \\ 1 & \cos(\psi_3) & \sin(\psi_3) \end{bmatrix} \begin{bmatrix} \theta_0(t) \\ \theta_{\text{tilt}}(t) \\ \theta_{\text{yaw}}(t) \end{bmatrix}. \tag{2}$$

The signals imposed through the MBC by the Helix approach are given as follows:

$$\theta_{\text{tilt}} = \alpha \sin(\omega_e t), \tag{3}$$
$$\theta_{\text{yaw}} = \alpha \sin(\omega_e t + \tau),$$

where α is the pitch amplitude in degrees, τ is the time delay in radians per second and $\omega_e = 2\pi f_e$ is the excitation frequency in radians per second. Applying these signals induces a yaw and tilt moment on the non-rotating coordinate frame, misaligning the direction of the thrust force from the rotor center in a dynamic fashion. Generally, a time delay of $\pi/2$ or $3\pi/2$ is selected, which generates a counterclockwise and a clockwise rotating wake, respectively. The amplitude is usually selected between 0.5 and 4 degrees. As the pitch angle oscillates with this amplitude around the optimal pitch value for a specific wind speed, an upper bound will likely be imposed in practice by the dynamic stall region. A lower bound might be set by the pitch bearing specifications, mitigating the risk for surface-induced damage on the bearing caused by small oscillations [25].

When the turbine is operating below rated at constant speed ω_r, the collective pitch $\theta_0 = 0$ and the azimuth ψ_i can be taken as $\omega_r t$. Then, if choosing $\tau = \pi/2$ and substituting (3) in (2) for a blade $\theta_i(t)$ for $i = 1, 2, 3$, yields:

$$\theta_b(t) = \begin{bmatrix} 1 & \cos(\psi_i) & \sin(\psi_i) \end{bmatrix} \begin{bmatrix} 0 \\ \alpha \sin(\omega_e t) \\ \alpha \cos(\omega_e t) \end{bmatrix}, \tag{4}$$
$$= \cos(\omega_r t + \psi_{0,i}) \sin(\omega_e t) + \sin(\omega_r t + \psi_{0,i}) \cos(\omega_e t),$$
$$= \sin((\omega_r + \omega_e)t + \psi_{0,i}),$$

from which it can be derived that the resulting pitch command has a frequency of $\omega_\theta = \omega_r + \omega_e$, with $\omega_e \ll \omega_r$. A similar derivation for clockwise Helix ($\tau = 3\pi/2$) can be performed, yielding a frequency of $\omega_\theta = \omega_r - \omega_e$.

The excitation frequency f_e is governed by the dimensionless Strouhal number S_t and scales with turbine rotor size D and ambient wind speed U_∞:

$$S_t = \frac{f_e D}{U_\infty}. \tag{5}$$

The Strouhal is generally taken between 0.1 and 1. Unlike for DIC, the Strouhal value yielding the highest power production for has not been formally determined yet. However, one study analysed a small number of cases and found 0.4 a suitable value [26].

B. Fatigue analysis

Fatigue is the damage that builds up in structures over time due to cyclic loading. This damage consists of small cracks that propagate gradually until reaching a point of failure. Structural parameters, such as the damping and natural frequencies, govern the magnitude of the responses to this cyclic loading. Therefore, having adequate knowledge of these parameters is important, as wind turbines are generally designed to withstand cyclic loading from their environment for at least 20 years [27].

The damaging effect of cyclic loading on a structure can be modelled using the S-N (or Wöhler) curve, which indicates the number of cycles a structure can endure until failure for the given stress through which it is cycled [3]. Its slope is used in the calculation of the damage equivalent load (DEL),
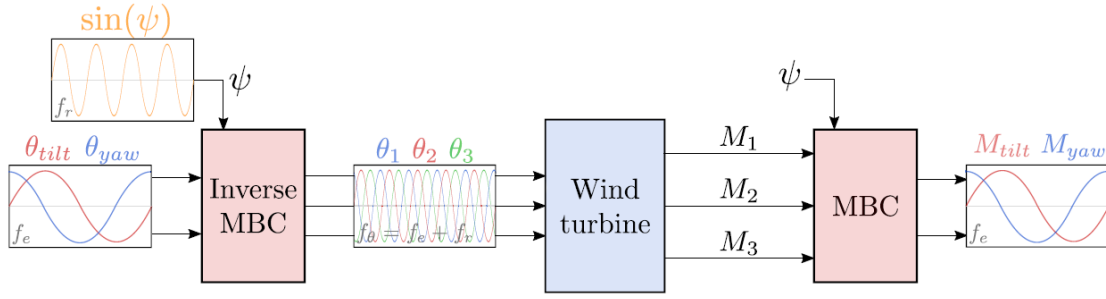
Fig. 1. Schematic of the MBC transform [19].

which encapsulates the total fatigue damage experienced by a structure in one single load, equivalent to the total damage of different load cycles experienced by that structure over time. Additionally, the DEL requires the ranges and frequencies of different load cycles, which can be extracted from a load signal using rainflow counting. To use these cycles in the DEL, the means need to be corrected to a single mean value. This is accomplished using the Goodman correction:

$$A_i^{\text{RF}} = A_i \left(\frac{A^{\text{u}} - |A^{\text{fm}}|}{A^{\text{u}} - |A_i^{\text{m}}|} \right), \tag{6}$$

where A_i^{RF} is the Goodman-corrected range, A_i is the range and A^{m} is the mean of the ith cycle, A^{u} is the ultimate load, and A^{m} is the chosen fixed mean load, set here as the mean of the entire signal.

The DEL is then calculated as follows:

$$DEL = \left(\frac{\sum_{i=1}^{N} (A_i^{\text{RF}})^m n_i}{n_{\text{eq}}} \right)^{\frac{1}{m}}, \tag{7}$$

where N is the total number of cycles, m is the inverse Wöhler slope taken conventionally as 5 for the tower and 10 for the blades, n_i is the number of cycles with range A_i, and n_{eq} the equivalent cycle, set here as 1. NREL's MLife toolbox was used to perform these calculations [28].

Observing the equation for DEL in (7), and considering that the Helix approach actuates the wind with oscillating pitch action (3), it is expected that Helix pitch action generates additional vibrations in the turbine which increase in magnitude with increasing Helix amplitude, thus contributing to the DEL. Moreover, as the DEL equation sums all cycles, it is also expected that the DEL increases with increasing Strouhal. In this study, the DELs are calculated for the following components:

- Blade Root Moment: Edgewise, Flapwise, and Torsional direction
- Tower Top Moment: Fore-aft, Side-side, and Torsional direction
- Tower Base Moment: Fore-aft and Side-side direction

C. Pitch Bearing Damage

Pitch bearing damage (PBD) is not quantified using rainflow counting. The standard used in this study is one prescribed by

bearing manufacturers and given by the following equation:

$$PBD(\phi) = \sum_{k=1}^{N} \delta\theta (\max(\cos(\phi)M_{\text{flap}} + \sin(\phi)M_{\text{edge}}, 0))^m, \tag{8}$$

where $\delta\theta$ is the pitch difference, ϕ is the radial position of the bearing, M_{flap} is the flapwise blade root bending moment, M_{edge} is the edgewise blade root bending moment, and m is the inverse Wöhler slope. In our analysis, the radial position with the largest damage is considered.

Analysing (8), PBD is expected to increase for higher frequent pitch action as pitch travel increases. This is the case for increasing Strouhal for CCW Helix and for decreasing Strouhal for CW Helix (See (4)).

III. SIMULATION SETUP

In this section, the simulation software and tools are presented. First, the analysed turbine, then the turbine controller, and ultimately a description of the simulation environment is given, along with the simulated controller parameters.

A. IEA-15MW offshore wind turbine

The turbine considered here is the fixed-bottom IEA-15MW reference offshore turbine with a radius of 120 m and a hub height of 150 m. The turbine is a direct-drive offshore wind turbine with a cut-in wind speed of 4 m/s, a rated wind speed of 10.59 m/s, and a rated RPM of 7.55. For a more elaborate description, the reader is referred to the technical report [29].

B. Controller

The IEA-15MW turbine is equipped with the reference open-source controller (ROSCO). This controller has state-of-the-art control capabilities, such as peak-shaving and individual pitch control [30].

Note that enhanced wake mixing is not expected to be economical in the above-rated regime as added loads increase and added power decreases due to the abundance of wind [18]. Practical implementation of the Helix approach will therefore most likely be confined to the below-rated region. Hence, the ROSCO controller is modified such that the Helix signal can be superimposed in region 2.

C. Simulation Environment

The IEA-15MW turbine with ROSCO + Helix controller is simulated in OpenFAST v3.1.0 [31], a well-established medium-fidelity aero-elastic wind turbine simulation tool.

The simulation sampling frequency is chosen as 200 Hz and lasts 900 seconds, where the first 300 s are discarded to remove transient effects. Furthermore, each simulation is run with 6 different turbulent wind seeds, whose calculated DELs are averaged to reduce variance. Simulations are conducted for the entire wind speed range in region 2 (3–10 m/s) using inflow with IEC normal turbulence model level C based on the IEC Kaimal spectral model. The Helix amplitude is varied between 0.25 and 4 degrees, and the Strouhal is varied between 0.1 and 1 for both clockwise and counterclockwise directions. Besides simulations with Helix control, baseline simulations are conducted to provide a comparison. Altogether, this totals 15,408 simulations that were computed on the Delft Blue high-performance computer using 1200 CPU cores [32]. A summary of the parameters is given in Table I.

TABLE I

OVERVIEW OF THE PARAMETER SETTINGS USED IN THE SIMULATIONS.

Parameter	Values	Steps
Wind speed	3 - 10 m/s	1
Strouhal	0.1 - 1	0.1
Amplitude	0.25 - 4 deg	0.25

IV. RESULTS

The DELs and PBD for the CW and CCW direction are presented in 3D surface plots in Fig. 2. The x- and y-axis represent the amplitude and Strouhal value used in the simulation. The z-axis shows the Helix DEL relative to the baseline DEL. For PBD, the z-axis shows the absolute value as a relative comparison would not be informative: almost no PBD builds up at below-rated wind speeds due to little pitch action. All results were averaged over 6 seeds and Weibull weighted across wind speeds. The CW surface plot has a red grid, the CCW surface plot has a black grid, and a colorbar indicates the magnitude of each DEL.

Each channel is qualitatively analysed in Table II. The sensitivity is rated ↑ - ↑↑↑↑, where ↑ is very low positive sensitivity (↓ for negative sensitivity) and ↑↑↑↑ is very high positive sensitivity; a '−' indicates negligible sensitivity.

From the results, it can be derived that the blade root flapwise, tower top fore-aft, tower torsional and PBD are very sensitive to Helix amplitude. This can be explained by the way Helix operates, which steers the thrust force to follow a circular pattern around the axis instead of being directed upwind. This enforcement increases blade vibrations, especially in the flapwise direction, and creates a fluctuating tilt and yaw moment due to deliberate misalignment with the wind direction, resulting in higher torsional and fore-aft loads in the top part of the tower.

TABLE II

SENSITIVITY OF THE DELs TO THE HELIX PARAMETERS.

Channel		Sens. to ↑ Amp.	Sens. to ↑ St
Blade Root Edgewise	CW	↑	−
	CCW	↑	−
Blade Root Flapwise	CW	↑↑↑↑	−
	CCW	↑↑↑↑	↓
Blade Root Torsional	CW	↑	↑
	CCW	↑	−
Tower Top Fore-Aft	CW	↑↑↑	↑↑↑
	CCW	↑↑↑	↑↑
Tower Top Side-Side	CW	↑↑	↑↑
	CCW	↑↑	↑
Tower Torsional	CW	↑↑↑	↑↑↑
	CCW	↑↑↑	↑↑
Tower Base Fore-Aft	CW	↑	↑
	CCW	↑	−
Tower Base Side-Side	CW	↑	−
	CCW	−	−
Pitch Bearing Damage	CW	↑↑↑↑	↓↓
	CCW	↑↑↑↑	↑

The channels with the largest sensitivity to Strouhal can be found on the tower. This could stem from the fact that a relative increase in Strouhal results in the same relative increase in load cycles on the tower due to Helix control, whereas the resultant frequency on the blades is $\omega_\theta = \omega_r \pm \omega_e$ due to the MBC transformation (4) resulting in a lower relative cycle increase for CCW and a cycle decrease for CW. This effect can be observed in greater detail in Fig. 3, where several power spectra, averaged over 6 seeds, are presented for different Strouhal settings. In the blade root flapwise channel for CW Helix, the Strouhal peak starts around the 0.1 Hz 1P frequency and decreases for higher Strouhal, while for CCW Helix, the opposite effect is observed. Higher harmonics can also be seen. The Helix peak in the tower top fore-aft channel starts around 0 Hz and increases linearly with Strouhal irrespective of the Helix direction.

Although the number of cycles decreases for CW Helix with increasing Strouhal, the tower DELs increase more compared to CCW Helix. It is difficult to see from power spectra, but it was found that the CW Helix peak has a stronger magnitude compared to CCW Helix: 93.3 versus 92.8 dB, indicating a higher amplitude of the resulting vibrations. For PBD, this is the opposite and can be derived from the fact that the pitch frequency (and hence the pitch difference $\delta\theta$, (8)) increases for CCW Helix and decreases for CW Helix with higher Strouhal.

Note that, although the load increases presented here seem significant, the Helix is expected to be active only 10-20% of the time in practice, as the main performance gain is achieved when the wake effect takes place, i.e. when the turbines are (partly) aligned with the wind direction. Therefore, the added loads should be discounted by this factor, meaning that a load increase of e.g. 30% with Helix activated results in an annual load increase of only 3-6%.
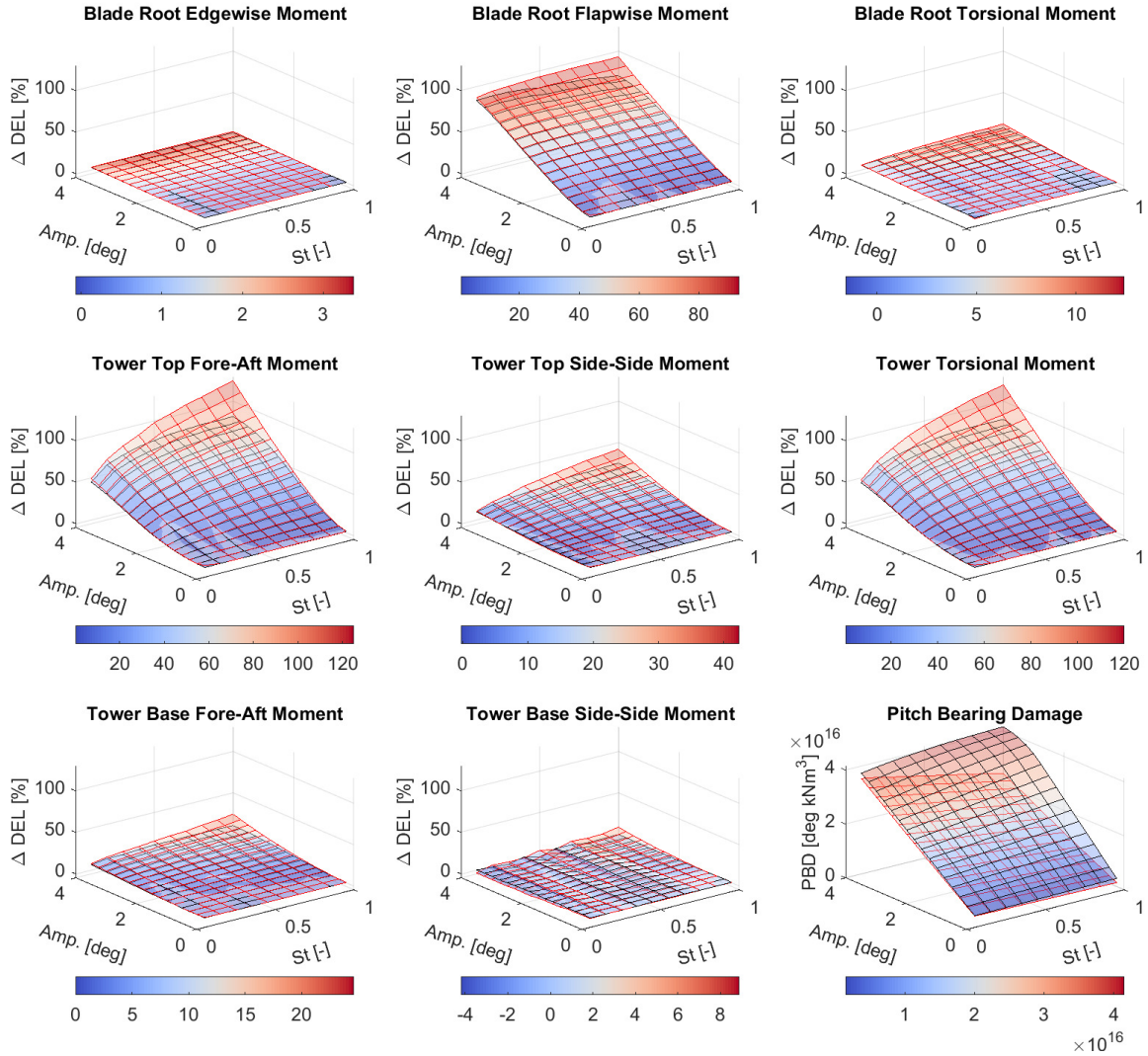
Fig. 2. 3D surface plots of all parameters simulated for Helix. Each plot presents the DEL relative to the baseline case for CW (red grid) and CCW (black grid) Helix. The x-axis and y-axis describe the different Helix settings, amplitude and Strouhal, respectively. The z-axis describes the relative DEL. Generally, the DELs are higher for CW.
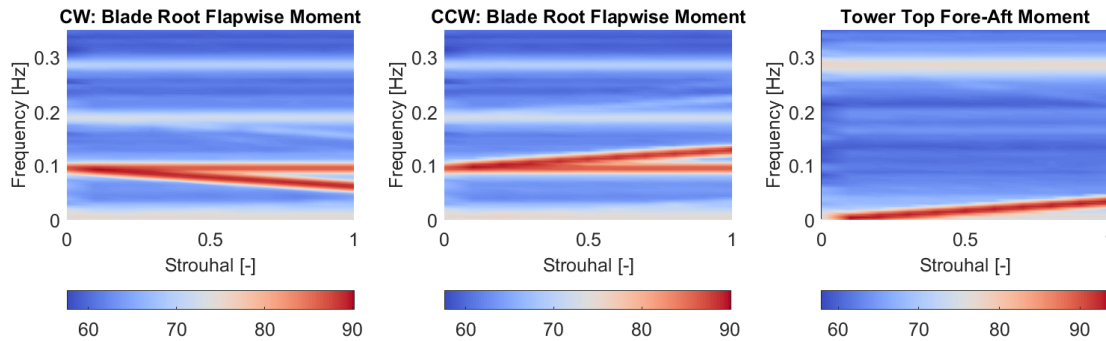

Fig. 3. Power spectra of several relevant load channels for increasing Strouhal. The resultant Helix excitation frequency decreases in the blade coordinate frame for CW Helix, whereas it increases for CCW Helix. In the tower coordinate frame, the frequencies are identical.

V. CONCLUSIONS

The Helix approach is a control strategy that increases wind farm performance by mitigating the wake effect through individual pitch control. This study found that increasing the amplitude of the excitation signal leads to notable increases in pitch bearing damage and turbine loads, particularly in the blade root flapwise, tower top fore-aft, and tower torsional direction. While higher amplitude may result in better wake mixing, further LES studies are needed to determine the trade-off with the loads increase. Loads were less affected by Strouhal, allowing more tuning freedom. The counter-clockwise Helix direction was found to cause lower loads, while also performing better in terms of AEP gain. The clockwise Helix direction requires less pitch action, which may be beneficial for turbines with pitch bearing actuation restrictions.

ACKNOWLEDGMENT

REFERENCES

[1] Ministerie van Algemene Zaken, "Kabinet verdubbelt productie windenergie op zee," Mar 2022. [Online]. Available: https://www.rijksoverheid.nl/actueel/nieuws/2022/03/18/kabinet-verdubbelt-productie-windenergie-op-zee

[2] ——, "Offshore wind energy," Jul 2021. [Online]. Available: https://www.government.nl/topics/renewable-energy/offshore-wind-energy

[3] T. Burton, N. Jenkins, D. Sharpe, and E. Bossanyi, *Wind energy handbook*. John Wiley & Sons, 2011.

[4] M. Adaramola and P.-Å. Krogstad, "Experimental investigation of wake effects on wind turbine performance," *Renewable energy*, vol. 36, no. 8, pp. 2078–2086, 2011.

[5] K. Thomsen and P. Sørensen, "Fatigue loads for wind turbines operating in wakes," *Journal of Wind Engineering and Industrial Aerodynamics*, vol. 80, no. 1-2, pp. 121–136, 1999.

[6] J. F. Manwell, J. G. McGowan, and A. L. Rogers, *Wind energy explained: theory, design and application*. John Wiley & Sons, 2010.

[7] K. Yang, G. Kwak, K. Cho, and J. Huh, "Wind farm layout optimization for wake effect uniformity," *Energy*, vol. 183, pp. 983–995, 2019.

[8] R. J. Barthelmie, K. Hansen, S. T. Frandsen, O. Rathmann, J. Schepers, W. Schlez, J. Phillips, K. Rados, A. Zervos, E. Politis, *et al.*, "Modelling and measuring flow and wind turbine wakes in large wind farms offshore," *Wind Energy*, vol. 12, no. 5, pp. 431–444, 2009.

[9] J. W. van Wingerden, P. A. Fleming, T. Göçmen, I. Eguinoa, B. Doekemeijer, K. Dykes, M. Lawson, E. Simley, J. King, D. Astrain, *et al.*, "Expert elicitation on wind farm control," in *Journal of Physics: Conference Series*, vol. 1618, no. 2. IOP Publishing, 2020, p. 022025.

[10] J. W. Wagenaar, L. Machielse, and J. Schepers, "Controlling wind in ECN's scaled wind farm," *Proc. Europe Premier Wind Energy Event*, vol. 1, no. 01, 2012.

[11] P. A. Fleming, P. M. Gebraad, S. Lee, J. W. van Wingerden, K. Johnson, M. Churchfield, J. Michalakes, P. Spalart, and P. Moriarty, "Evaluating techniques for redirecting turbine wakes using sowfa," *Renewable Energy*, vol. 70, pp. 211–218, 2014.

[12] J. Annoni, P. M. Gebraad, A. K. Scholbrock, P. A. Fleming, and J. W. v. Wingerden, "Analysis of axial-induction-based wind plant control using an engineering and a high-order wind plant model," *Wind Energy*, vol. 19, no. 6, pp. 1135–1150, 2016.

[13] D. van der Hoek, S. Kanev, J. Allin, D. Bieniek, and N. Mittelmeier, "Effects of axial induction control on wind farm energy production-a field test," *Renewable energy*, vol. 140, pp. 994–1003, 2019.

[14] J. P. Goit and J. Meyers, "Optimal control of energy extraction in wind-farm boundary layers," *Journal of Fluid Mechanics*, vol. 768, pp. 5–50, 2015.

[15] D. van der Hoek, J. Frederik, M. Huang, F. Scarano, C. Simao Ferreira, and J. W. van Wingerden, "Experimental analysis of the effect of dynamic induction control on a wind turbine wake," *Wind Energy Science*, vol. 7, no. 3, pp. 1305–1320, 2022.

[16] J. A. Frederik, R. Weber, S. Cacciola, F. Campagnolo, A. Croce, C. Bottasso, and J. W. van Wingerden, "Periodic dynamic induction control of wind farms: proving the potential in simulations and wind tunnel experiments," *Wind Energy Science*, vol. 5, no. 1, pp. 245–257, 2020.

[17] W. Munters and J. Meyers, "Towards practical dynamic induction control of wind farms: analysis of optimally controlled wind-farm boundary layers and sinusoidal induction control of first-row turbines," *Wind Energy Science*, vol. 3, no. 1, pp. 409–425, 2018.

[18] J. A. Frederik and J. W. van Wingerden, "On the load impact of dynamic wind farm wake mixing strategies," *Renewable Energy*, 2022.

[19] J. A. Frederik, B. M. Doekemeijer, S. P. Mulders, and J. W. van Wingerden, "The helix approach: Using dynamic individual pitch control to enhance wake mixing in wind farms," *Wind Energy*, vol. 23, no. 8, pp. 1739–1751, 2020.

[20] IEC 61400-3: 2019, "Wind energy generation system—part," International Electrotechnical Commission, Geneva, CH, Standard, 2019.

[21] E. A. Bossanyi, "Individual blade pitch control for load reduction," *Wind Energy*, vol. 6, no. 2, pp. 119–128, 2003.

[22] K. Selvam, S. Kanev, J. W. van Wingerden, T. van Engelen, and M. Verhaegen, "Feedback–feedforward individual pitch control for wind turbine load reduction," *International Journal of Robust and Nonlinear Control*, vol. 19, no. 1, pp. 72–91, 2009.

[23] G. Bir, "Multi-blade coordinate transformation and its application to wind turbine analysis," in *46th AIAA aerospace sciences meeting and exhibit*, 2008, p. 1300.

[24] S. P. Mulders, A. K. Pamososuryo, G. E. Disario, and J.-W. v. Wingerden, "Analysis and optimal individual pitch control decoupling by inclusion of an azimuth offset in the multiblade coordinate transformation," *Wind Energy*, vol. 22, no. 3, pp. 341–359, 2019.

[25] M. Stammler, A. Reuter, and G. Poll, "Cycle counting of roller bearing oscillations–case study of wind turbine individual pitching system," *Renewable Energy Focus*, vol. 25, pp. 40–47, 2018.

[26] C. Muscari, P. Schito, A. Viré, A. Zasso, D. van der Hoek, and J. W. van Wingerden, "Physics informed dmd for periodic dynamic induction control of wind farms," in *Journal of Physics: Conference Series*, vol. 2265, no. 2. IOP Publishing, 2022, p. 022057.

[27] A. A. W. van Vondelen, S. T. Navalkar, A. Iliopoulos, D. C. van der Hoek, and J. W. van Wingerden, "Damping identification of offshore wind turbines using operational modal analysis: A review," *Wind Energy Science*, vol. 7, no. 1, pp. 161–184, 2022.

[28] G. Hayman, "Mlife theory manual for version 1.00," *National Renewable Energy Laboratory, Golden, CO*, vol. 74, no. 75, p. 106, 2012.

[29] E. Gaertner, J. Rinker, L. Sethuraman, F. Zahle, B. Anderson, G. Barter, N. Abbas, F. Meng, P. Bortolotti, W. Skrzypinski, G. Scott, R. Feil, H. Bredmose, K. Dykes, M. Sheilds, C. Allen, and A. Viselli, "Definition of the IEA 15-megawatt offshore reference wind turbine," NREL/TP-75698, International Energy Agency, Tech. Rep., 2020. [Online]. Available: https://www.nrel.gov/docs/fy20osti/75698.pdf

[30] N. J. Abbas, D. S. Zalkind, L. Pao, and A. Wright, "A reference open-source controller for fixed and floating offshore wind turbines," *Wind Energy Science*, vol. 7, no. 1, pp. 53–73, 2022.

[31] J. Jonkman, "The new modularization framework for the fast wind turbine cae tool," in *51st AIAA aerospace sciences meeting including the new horizons forum and aerospace exposition*, 2013, p. 202.

[32] Delft High Performance Computing Centre (DHPC), "DelftBlue Supercomputer (Phase 1)," https://www.tudelft.nl/dhpc/ark:/44463/DelftBluePhase1, 2022.